THE JOURNAL OF BIOLOGICAL CHEMISTRY VOL. 291, NO. 43, pp. 22534–22543, October 21, 2016

Lipids Activate SecA for High Affinity Binding to the SecYEG Complex*

Received for publication, June 17, 2016, and in revised form, August 30, 2016 Published, JBC Papers in Press, September 9, 2016, DOI 10.1074/jbc.M116.743831

Sabrina Koch[‡], Janny G. de Wit[‡], Iuliia Vos[‡], Jan Peter Birkner[§], Pavlo Gordiichuk[¶1], Andreas Herrmann[¶], Antoine M. van Oijen[§‖], and Arnold J. M. Driessen[‡2]

From the [‡]Molecular Microbiology, Groningen Biomolecular Sciences and Biotechnology Institute and Zernike Institute for Advanced Materials and the [§]Single-molecule Biophysics, Zernike Institute for Advanced Materials, University of Groningen, 9747 AG Groningen, The Netherlands, the [¶]Polymer Chemistry and Bioengineering, Zernike Institute for Advanced Materials, 9747 AG, Groningen, The Netherlands, and the [‖]School of Chemistry, University of Wollongong, Wollongong, New South Wales 2522, Australia

Protein translocation across the bacterial cytoplasmic membrane is an essential process catalyzed predominantly by the Sec translocase. This system consists of the membrane-embedded protein-conducting channel SecYEG, the motor ATPase SecA, and the heterotrimeric SecDFyajC membrane protein complex. Previous studies suggest that anionic lipids are essential for SecA activity and that the N terminus of SecA is capable of penetrating the lipid bilayer. The role of lipid binding, however, has remained elusive. By employing differently sized nanodiscs reconstituted with single SecYEG complexes and comprising varying amounts of lipids, we establish that SecA gains access to the SecYEG complex via a lipid-bound intermediate state, whereas acidic phospholipids allosterically activate SecA for ATP-dependent protein translocation.

Approximately 25–30% of bacterial proteins are embedded in the cytoplasmic membrane or carry out their distinct functions outside the cell. The majority of these proteins are synthesized at ribosomes in the cytoplasm and directed to the Sec translocase, the major platform for translocation across and insertion into the cytoplasmic membrane (1). Proteins are targeted to the Sec translocase either post-translationally by their N-terminal signal sequence or co-translationally as ribosome nascent chains. During post-translational targeting, secretory proteins are captured by the cytoplasmic chaperone SecB, which prevents premature (mis)folding and degradation and keeps the preprotein in a translocation competent state (2). The SecB-preprotein complex is bound by SecA, which in turn interacts with the heterotrimeric protein conducting channel SecYEG. SecA is a multiple domain protein and enables protein translocation via ATP hydrolysis (3) through its interactions with the SecYEG complex and unfolded secretory proteins. It has been proposed that SecA directs secretory proteins into the SecYEG pore via two short helices (two-helix finger) (4).

The exact targeting mechanism of SecA to the membrane and the dynamics of its interaction with the SecYEG channel are poorly understood. Studies using cell fractions have shown that SecA cycles between the cytosol and the cytoplasmic membrane (5), which was suggested to be ATP-dependent (6). As shown with liposomes, SecA binds with low affinity to lipids, a process that is enhanced by the presence of negatively charged lipids (7, 8). In contrast, no binding was found to inner membrane vesicles (IMVs)[3] that lack the negatively charged lipid phosphatidylglycerol (7). In the free soluble state, SecA is inactive for ATP hydrolysis and exhibits only poor peptide binding (7). In the lipid-bound state, SecA is thermolabile but is stabilized by the presence of unfolded secretory proteins, an activity that is termed SecA lipid ATPase. SecA binds with high affinity to the membrane-embedded SecYEG complex (K_D = 4.5 nM) (9), but it shows only low affinity binding to the detergent-solubilized SecYEG (3.9 μM) (10). Important, acidic phospholipids such as phosphatidylglycerol are essential for protein translocation. *In vitro*, the signal sequence of secretory proteins have been shown to bind, fold, and penetrate membranes containing acidic phospholipids. These experiments indicate that not only the presence but also the type of lipid might play a role in the targeting and/or functioning of SecA to the membrane, but an exact role for lipid binding has never been demonstrated.

The crystal structure of the SecA-SecY complex in solution has provided new insights into the binding mechanism of SecA (4). Binding mostly occurs through cytosolic loops 6–7 and 8–9 of SecY via electrostatic interactions to the polypeptide-cross-linking and helical scaffold domains of SecA. However, there are no distinct interactions with phospholipids that emerge from the structure. The SecA N terminus was shown earlier to be involved in lipid binding (11). This N terminus is not conserved, but its highly amphipathic nature is omnipresent. Because of its net positive charge, this region of SecA is predicted to be membrane surface seeking interacting with

* This work was supported by the Stichting voor Fundamenteel Onderzoek der Materie (FOM). The authors declare that they have no conflicts of interest with the contents of this article.
[1] Present address: Dept. of Chemistry, Northwestern University, Evanston, IL.
[2] To whom correspondence should be addressed: Molecular Microbiology, Groningen Biomolecular Sciences and Biotechnology Institute and Zernike Institute for Advanced Materials, Nijenborgh 7, 9747 AG Groningen, The Netherlands. Tel.: 31-50-3632164; Fax: 31-50-3632154; E-mail: a.j.m.driessen@rug.nl.

[3] The abbreviations used are: IMV, inner membrane vesicle; OmpA, outer membrane protein A; DHFR, dihydrofolate reductase; Apo, apolipoprotein; MSP, major scaffold protein; DOPC, 1,2-dioleoyl-*sn*-glycero-3-phosphocholine; DOPG, 1,2-dioleoyl-*sn*-glycero-3-phosphoglycerol; DOPE, 1,2-dioleoyl-*sn*-glycero-3-phosphoethanolamine; SEC, size exclusion chromatography; AFM, atomic force microscopy; MST, microscale thermophoresis; FCCS, fluorescence cross-correlation spectroscopy; NTA, nitrilotriacetic acid.

acidic phospholipids (12). Deletion of the N terminus results in the inactivation of SecA, but activity can be restored by replacing the N terminus with a His tag and supplementing SecYEG proteoliposomes with Ni^{+}-NTA lipids, suggesting that membrane tethering is important for functioning (11). In the SecA-SecY structure, however, the helical amphipathic N terminus of SecA is positioned away from where the membrane would be located, and a major conformational change involving a 30 Å translational movement would be required to allow this region to deeply penetrate the membrane, which could potentially impact the SecY binding mode and SecA function. This N-terminal displacement of SecA suggests not only a tethering function of the N terminus but also a key role function in conformational activation of SecA upon lipid binding.

Earlier studies have shown that the presence of negatively charged lipids is essential for the activity of the Sec translocase. However, the actual role of the lipid bilayer in the translocation process remained to be elucidated. Here, we have used two different sizes of nanodiscs harboring single SecYEG complexes surrounded by different quantities of lipids to study the functional interaction between SecYEG and SecA. Our data suggest that high affinity binding of SecA to SecYEG is dependent on the presence of bulk acidic phospholipids. We further show not only that the SecA N terminus that interacts with acidic phospholipids is important to tether SecA to the membrane but also that this binding event induces a conformational change of SecA that promotes its interactions with SecYEG. Our data suggest that the lipid bound SecA is a true intermediate in the catalytic cycle and provides an explanation why SecA is primed for high affinity SecYEG binding upon its interaction with acidic phospholipids. We propose a new mechanism of protein translocation, whereby SecA first binds acidic phospholipids in the membrane whereupon the lipid bound SecA intermediate interacts with SecYEG with high affinity.

Results

Formation of SecYEG-containing Small and Large Nanodiscs—To examine the influence of phospholipids on the reconstituted SecA-SecYEG complex, two different nanodisc systems were employed. Nanodiscs are lipid patches that are formed by a protein belt, *i.e.* a scaffold protein. By changing the scaffold protein, the size and therefore the amount of lipids in the nanodisc can be changed (Fig. 1). To generate small nanodiscs, the membrane scaffold protein MSP1E3D1 (13) was used. This scaffold protein is derived from the apolipoprotein A-1 and forms a two-copy helical belt, yielding discs of ~13 nm (13). In contrast, for large nanodiscs, the scaffold protein ApoE422k, which is the 22-kDa fragment of apolipoprotein E-4, was employed (14). For this scaffold protein, nanodiscs sizing from 14.5 to 28 nm have been reported (15). Importantly, with ApoE422k, the ratio of scaffold protein to lipid determines the disc size. Computer simulations have shown that each additional copy of ApoE422k increases the disc diameter by ~4.5 nm (15). By using both nanodiscs systems, it is possible to generate compartments where the SecYEG channel is embedded by low or high lipid quantities, respectively (See below). In the nanodiscs, the copy number of reconstituted SecYEG per disc can be determined via Poisson distribution. Because single

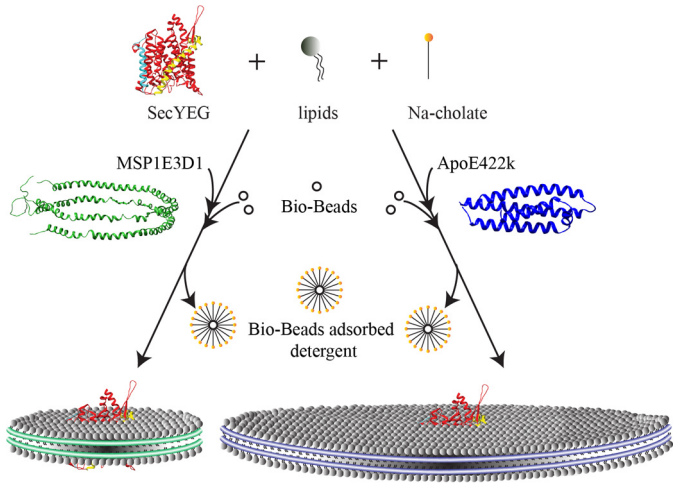

FIGURE 1. **Schematic workflow of nanodisc preparation.** Detergent-solubilized SecYEG was mixed with lipids and the detergent sodium cholate. Scaffold proteins MSP1E3D1 or ApoE422k were added to form small or large nanodiscs, respectively. The formation of discs was initiated by removal of detergent using biobeads. SecYEG small and large discs are drawn on relative scale.

SecYEG complexes are sufficient for protein translocation (16), a SecYEG to lipid molar ratio (0.25:1800) was chosen that favors the formation of discs with single SecYEG complexes. This method was used previously for the small nanodiscs (17), but the increased size of the large nanodiscs caused us to ascertain the above assumption experimentally. According to the molar ratio and ~1100 lipid molecules/31-nm nanodisc (assuming 8 copies of ApoE422K (15)), 16% of the discs are expected to contain a single copy, whereas 80% will be empty, and less than 3% will contain multiple copies of SecYEG, as shown previously (18). Nanodiscs were formed using sodium cholate as described (19), with a lipid composition of DOPC:DOPE:DOPG (40:30:30 molar ratio) (16). Small and large nanodiscs were subjected to size exclusion chromatography (SEC) and analyzed by SDS-PAGE. Peak fractions (fractions 19–26 for large discs and fractions 29–34 for small discs) were pooled (Fig. 2*A*) and further analyzed by atomic force microscopy (AFM) (Fig. 2*B*). The diameters of the discs ($n = 200$ for both large and small discs) were analyzed, plotted in a histogram, and fitted to a Gaussian model (Fig. 2*C*). The mean diameter of the small nanodiscs was found to be ~12.7 nm ($\sigma = 4$ nm), which is consistent with data from previous studies (13). The diameter of the large nanodiscs was found to be 31 nm ($\sigma = 9$ nm). To demonstrate that the discs consist of a lipid bilayer, the height of large discs was measured ($n = 200$) (Fig. 2*D*). On average, the discs had a thickness of 3.8 nm ($\sigma = 0.3$ nm). Considering that the lipids used in this study had a acyl chain length of 18 carbon atoms, the thickness value is in good agreement with the expected values for single lipid bilayers (20). Moreover by AFM, the presence of SecYEG complexes was detected being evident because of an increase in height, which could represent the periplasmic or cytoplasmic loop of SecYEG (21) (Fig. 2*E*). Examination of a set of large nanodiscs ($n = 200$) showed that 14.5% of the discs showed such elevations, which is in agreement with the theoretical expected distribution of single SecYEG complexes over the nanodiscs (Fig. 2*D*). With the experimentally determined average sizes of the small and large nanodiscs of 12.7 and 31 nm,

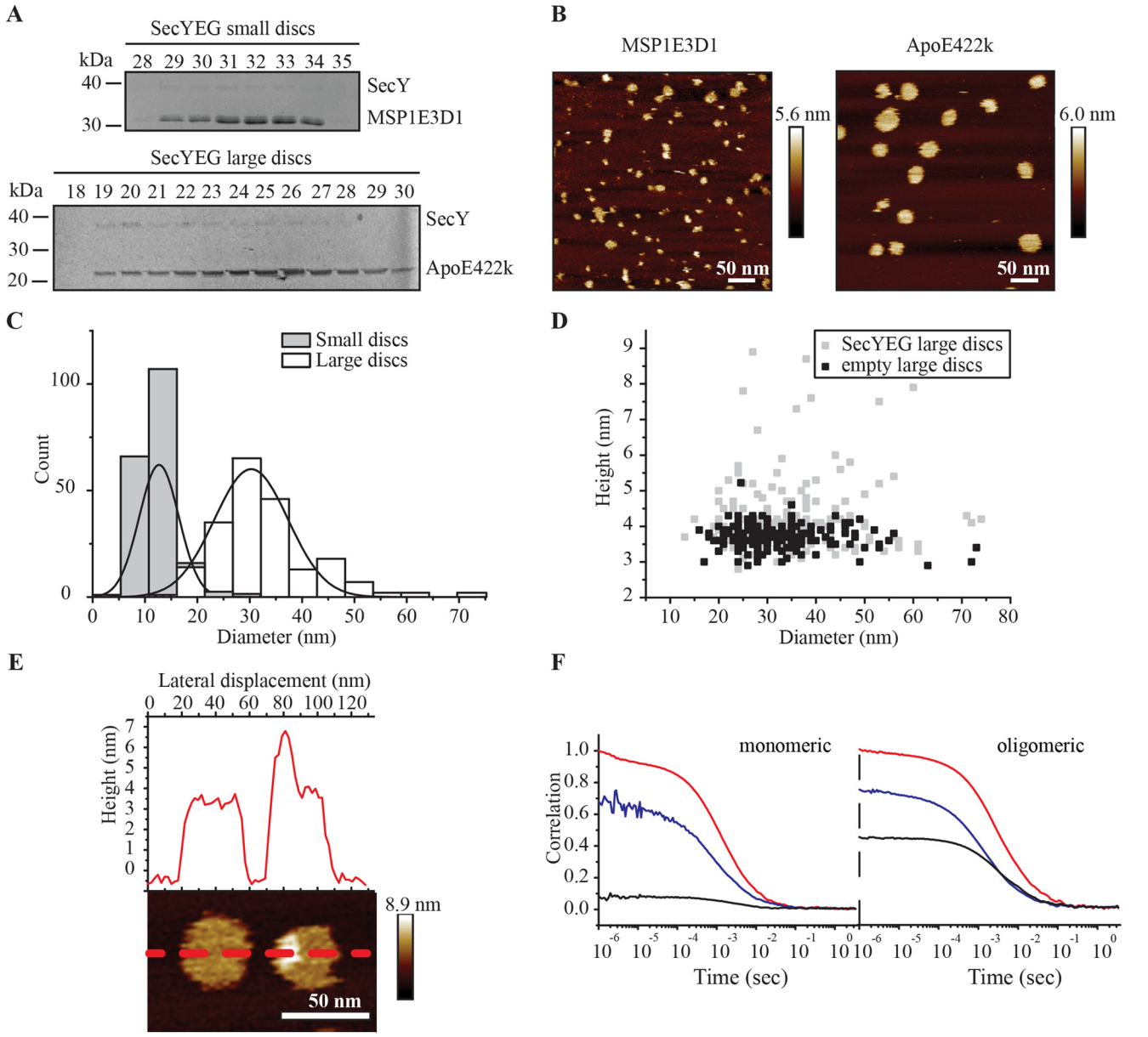

FIGURE 2. **Preparation of SecY$_{C148}$EG small and large nanodiscs.** *A*, single detergent-solubilized SecY$_{C148}$EG complexes were reconstituted into small and large nanodiscs. *B*, nanodiscs were subjected to size exclusion chromatography and visualized by atomic force microscopy. The *scale bars* represent a lateral scale of 50 nm. The *color-coded bars* on the *right side* represent height scales. *C*, the diameter of small ($n = 200$) (*gray*) and large nanodiscs ($n = 200$) (*white*) was measured, and the size distribution was plotted in a histogram. The centers of gravity were found at 12.7 and 31 nm for small and large discs, respectively. *D*, the height of empty (*black*) and SecYEG (*gray*) large discs were plotted against their corresponding diameter. On average the discs have a height of 3.8 nm, which increases in the presence of SecYEG. *E*, the cross-section through an empty, and SecYEG large disc shows an increase of height caused by the cytoplasmic or periplasmic loop of SecYEG. *F*, FCCS analysis of the oligomeric state of SecYEG in large discs. SecY$_{C148}$EG was simultaneously labeled with Atto647N (*red*) and AlexaFluor 488 (*blue*) and reconstituted into large nanodiscs. The autocorrelation of the fluorescence of both fluorophores was recorded, and the cross-correlation (*black*) was determined. To ensure a monomeric state, SecYEG, ApoE422k, and lipids were mixed in a molar ratio of 0.25:10:1800. The monomeric state of SecYEG in the discs was confirmed by a low cross-correlation. In contrast the oligomeric state, represented by high cross-correlation, was achieved when the amount of SecYEG was increased using SecYEG, ApoE422k, and lipid molar ratio of 1:10:1800.

the number of lipids present in these discs amounts to ~160 and 1100, respectively, assuming 0.6 nm^2 as the lipid head surface area (22). To account for the space occupied by single SecYEG complexes, small and large SecYEG nanodiscs contain 120 and 1060 lipids, respectively, assuming a surface area of 20 nm^2 for the SecYEG channel.

To further validate the monomeric state of the SecYEG complexes in the large nanodiscs, Fluorescence cross-correlation spectroscopy (FCCS) was performed. Herein, SecY$_{C148}$EG was exposed in the label reaction to Atto647N and Alexa Fluor488 to ensure that each complex had either one or the other attached to it with equal probability. The labeled complexes were reconstituted into large nanodiscs as reported previously for small nanodiscs (17). The autocorrelation of the fluorescence of both fluorophores was recorded in a laser scanning LSM710 inverted confocal microscope. The cross-correlation in the large discs was less than 10%, representing a monomeric state of SecYEG (17) taking into account the low level of non-specific double labeling of SecY (see "Materials and Methods"). When the amount of SecYEG was increased in the reconstitu-

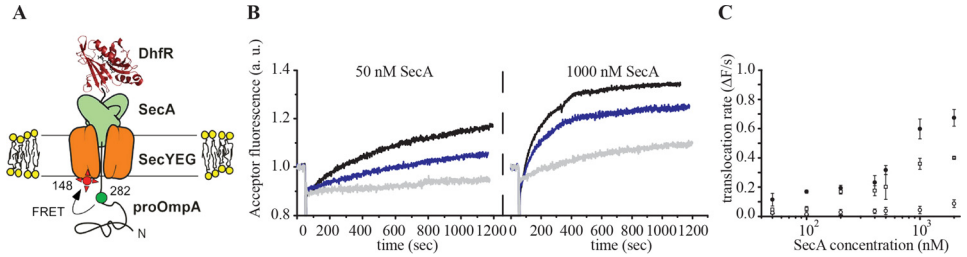

FIGURE 3. **Large lipid surface enhances SecA-dependent translocation.** *A*, principle of real time FRET-based assay. The prefolded DHFR domain fused to the precursor protein proOmpA cannot be translocated via the SecYEG pore, which stalls translocation and brings the donor-acceptor pair in close proximity for efficient FRET. *B*, SecYEG proteoliposomes (*black*), SecYEG large discs (*blue*), or SecYEG small discs (*gray*) were incubated in the presence of Cy3-conjugated proOmpA-DHFR and 50 nM (*left panel*) or 1000 nM (*right panel*) SecA. Translocation was initiated by the addition of ATP, and the formation of a stable SecYEG-preprotein intermediate was recorded following the acceptor fluorescence. *C*, ProOmpA translocation as a function of SecA concentration using SecYEG proteoliposomes (*black circles*), SecYEG large discs (*white squares*), or SecYEG small discs (*white circles*). The acceptor fluorescence signal after addition of ATP (time window $t = 70–120$ s) was plotted against a logarithmic time scale, and data points were fitted linearly with the equation $y = a + bx$, where a represents initial intensity with b as translocation rate. The translocation rate was plotted against the SecA concentration. Large nanodiscs are highly active and support translocation at low SecA concentrations (50 nM), whereas small nanodiscs need a very high SecA concentration (~1–2 μM).

tion mix, a cross-correlation, and therefore an oligomeric state, was detected (Fig. 2*F*). Both the AFM and FCCS experiments therefore demonstrate the presence of single SecYEG complexes in the large nanodiscs.

Translocation Is Dependent on the Lipid Surface—To study the influence of the available lipid surface on the translocation efficiency, the SecA-dependent translocation by SecYEG reconstituted into small and large nanodiscs was measured using a FRET-based translocation assay (16). Herein, the preprotein proOmpA fused at its C terminus to a dihydrofolate reductase (DHFR) domain was used. This domain can be folded in the presence of methotrexate and NADPH, so that the translocation of proOmpA-DHFR via SecYEG is stalled as the bulky, folded DHFR domain blocks further translocation. The unique cysteine at position 282 of proOmpA-DHFR and Cys^{148} at the periplasmic side of SecYEG were labeled with the FRET pair Cy3 and Atto647N, respectively. When both fluorophores get in close proximity, an increase of the FRET signal is detected reminiscent of translocation in the compartment-less system (Fig. 3*A*). SecYEG proteoliposomes and SecYEG reconstituted in small or large were incubated with fluorophore-conjugated proOmpA-DHFR and SecA until a steady fluorescent signal was achieved. Translocation was initiated by addition of 2 mM ATP, which resulted in the formation of a SecYEG-preprotein translocation intermediate as evidenced by an increase of the acceptor fluorescence (Fig. 3*B*). As expected, FRET was strictly dependent on the presence of ATP and SecA (data not shown) (16). Both nanodiscs support translocation, but with SecYEG reconstituted in the large nanodiscs, already low SecA concentrations (~50 nM) sufficed to observe an efficient FRET signal. This concentration of SecA compares favorable with the SecA dependence of protein translocation in SecYEG proteoliposomes (23). In contrast, for SecYEG-containing small nanodiscs, very high SecA concentrations (~1 μM) were needed to obtain a FRET signal indicating very inefficient translocation (Fig. 3*C*). These data suggest that the presence of a larger available lipid surface in the large nanodiscs allows for efficient translocation.

SecA Binding to SecYEG Is Dependent on the Lipid Surface—To determine whether the translocation deficiency of SecYEG in small discs was due to an impeded interaction of SecA with SecYEG, the SecA-SecYEG binding was determined using microscale thermophoresis (MST). With this method, the movement of a fluorescently labeled molecule along a temperature gradient is traced. By applying heat to these molecules, their hydration entropy decreases, which results in an enhanced diffusion out of the heated spot. This effect can be monitored by a decrease of fluorescence in the heated area. When adding a binding partner, the hydration of the fluorescently labeled protein will change, resulting in a different movement along the temperature gradient, which can be detected by an altered, usually slower decrease of fluorescence. Such binding events can be transformed into a binding curve. To employ the MST method, fluorescently labeled SecYEG in small or large nanodiscs was titrated with increasing amounts of SecA, and the temperature gradient movement of the nanodiscs was traced (Fig. 4*A*). SecA binds with high affinity to SecYEG present in large nanodiscs (K_D ~ 300 nM) with a Hill coefficient of 1, indicating a noncooperative binding between one SecA dimer and one SecYEG complex. In contrast SecA binding to SecYEG in small nanodiscs occurred with a very low affinity (K_D = ~3 μM). Instead of the synthetic lipid mixture, SecYEG was reconstituted in large nanodiscs comprising native *Escherichia coli* lipids. Binding of SecA to SecYEG in native lipids was slightly less efficient compared with the synthetic lipid mixture DOPC:DOPE:DOPG (40:30:30 molar ratio) (Fig. 4*A*). No SecA binding was detected, when SecYEG large discs were used that lacked the anionic lipid DOPG, DOPC:DOPE (40:60, molar ratio). This is in good agreement with earlier studies showing that anionic lipids are essential for protein translocation (7, 8).

To investigate the SecA binding in the absence of SecYEG, the ApoE422k was fluorescently labeled. Now a linear increase of the binding to large nanodiscs was observed, which did not saturate (Fig. 4*B*). The nonsaturating binding behavior of SecA suggests nonspecific lipid binding. Taken together, these results indicate that the available lipid surface is an important factor in high affinity SecA-SecYEG binding.

Lipids Induce a Conformational Change to SecA to Prime It for High Affinity SecYEG Binding—Previously, it was shown that the N terminus of SecA binds acidic phospholipids (11, 12) and is capable of penetrating the lipid bilayer (24) to function solely to tether the SecA to the lipid bilayer (11). However, in the *Thermotoga maritima* SecA-SecYEG complex structure in detergent, the N terminus of SecA is positioned such that it

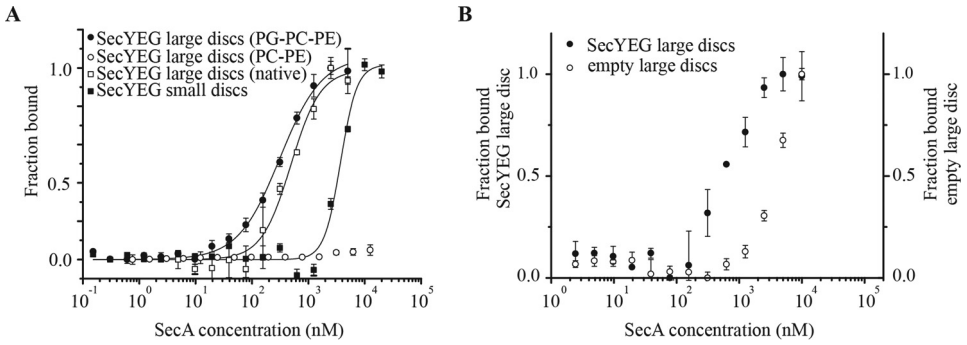

FIGURE 4. **SecA-SecYEG binding affinity is dependent on lipid surface area.** MST was performed to measure the binding of SecA to nanodiscs. *A*, SecA binding curves of SecYEG reconstituted in small (*black squares*) or large (*black* and *white circles* and *white squares*) nanodiscs as a function of the SecA concentration. With the large nanodiscs, the lipid composition was changed showing SecYEG in native *E. coli* lipids (*white squares*), DOPG:DOPC:DOPE, 30:40:30 (molar ratio) (*black circles*), and DOPC:DOPE, 40:60 (molar ratio) (*white circles*). *B*, SecA binding curves of lipid-filled (*white circles*) and SecYEG-reconstituted (*black circles*) large discs as a function the SecA concentration. Although SecA binds to empty discs in a nonsaturable manner (linear) up to 10 μM SecA, the interaction with SecYEG discs remains specific (sigmoidal). The experiments were performed in triplicate.

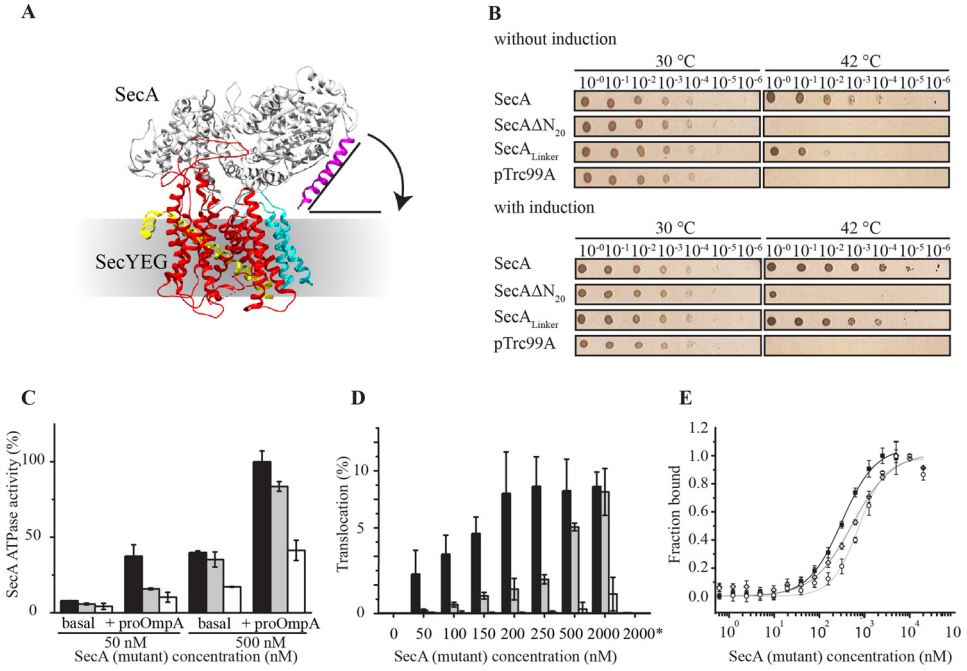

FIGURE 5. **The SecA N terminus allosterically activates SecA for high affinity binding to SecYEG.** *A*, side view of the *T. maritima* SecA-SecYEG complex (4). The trimeric SecYEG complex is highlighted in *red*, *yellow*, and *blue*, respectively. The N terminus of SecA (*gray*) is highlighted in *magenta* and demonstrates the remote location from the membrane. To penetrate the membrane, the N terminus would have to perform an ~30 Å translational movement (*arrow*). *B*, *E. coli* BL21.19 temperature-sensitive *secA* strain, expressing plasmid-borne SecA mutants, was grown at permissive (30 °C) or nonpermissive (42 °C) temperature. When overexpressed (*lower panel*), SecA and a $SecA_{Linker}$ could rescue the phenotype at the nonpermissive temperature. $SecA\Delta N_{20}$ is inactive but also complements when overexpressed at a low level. *C*, SecA (variant) sample was supplemented with SecYEG proteoliposomes, and the ATPase activity was measured in the absence and the presence of proOmpA. $SecA_{Linker}$ (*gray bars*) shows low enzymatic activity at low concentrations (50 nM) but close to wild type (*black bars*) activity at high concentrations (500 nM). In contrast, even at high concentrations, the N-terminal deleted SecA (*white bars*) barely shows activity. Wild type activity of 100% refers to an activity of 4.8 nmol/min. *D*, the SecA-dependent translocation of proOmpA into SecYEG proteoliposomes was plotted against the SecA concentration. $SecA_{Linker}$ (*gray bars*) shows a low translocation activity at low concentrations but wild type (*black bars*) activity at 2000 nM. The N-terminal deletion (*white bar*) of SecA disrupts its function. The *asterisk* represents the SecYEG proteoliposome sample that lacked the polar lipid DOPG, which caused a translocation deficiency for SecA (mutants). *E*, MST-based SecA binding curves to SecYEG large discs for the wild type SecA (*black squares*), $SecA_{Linker}$ (*dark gray diamonds*), and $SecA\Delta N_{20}$ (*light gray circles*). Although $SecA_{Linker}$ and $SecA\Delta N_{20}$ show a decrease in binding affinity, they showed saturation of binding at very high concentrations. The experiments were performed in triplicate.

would not contact the lipid bilayer (Fig. 5*A*). A relocation of the N terminus to the lipid bilayer can occur only when SecA undergoes a large conformational change. To discriminate between a tethering function and a conformational change, we designed a SecA mutant harboring a 10-amino acid linker after the first 20 amino acids of the N terminus ($SecA_{Linker}$). If the N terminus is solely responsible for membrane tethering, the linker insertion should not affect the activity. In contrast, the linker would disrupt a lipid induced conformational function of the N terminus. Plasmids bearing wild type SecA, $SecA_{Linker}$, and the N-terminal truncated $SecA\Delta N_{20}$, which was previously shown to be inactive (11), were transformed into *E. coli* BL21.19 to test for complementation of the SecA function (Table 1). This strain harbors a *secA Ts* mutation and is not viable at non-permissive temperatures (42 °C), whereas growth can be restored by a plasmid-based SecA expression. Although the $SecA_{Linker}$ mutant was able to complement the SecA deficiency, it did so with a much lower efficiency than the wild type SecA.

TABLE 1
Strains and plasmids used

Strain/plasmid	Description	Source
***E. coli* strain**		
DH5α	F−, *endA1, glnV44, thi-1, recA1, relA1, gyrA96, deoR, nupG, ϕ80dlacZΔM15,* Δ (*lacZYA-argF*)*U169, hsdR17* (*rK* − *mK*+), λ−	Ref. 41
SF100	F−, *lacX74, galE, galK, thi, rpsL* (*strA*), Δ*phoA*(*pvuII*), Δ*ompT*	Ref. 42
BL21 (DE3)	F− *omp*T *hsd*SB (rB−, mB−) *gal dcm* (DE3)	Ref. 43
BL21.19	*secA13*(*Am*) *supF*(*Ts*) *trp*(*Am*)*zch*::*Tn10 recA*::*CAT clpA*::*KAN*	Ref. 44
Plasmids		
pEK20-C148	SecY (L148C)EG	Ref. 16
pET504	proOmpA (S282C;C290S;C302S)-DhfR (C334S)	Ref. 38
pMKL 18	*E. coli* SecA under control of *lac* promoter/operator	Ref. 32
pTrc99 SecA	Wild type SecA	This study
pTrc99 SecA ΔN20	SecA with N-terminal 20-amino acid deletion	This study
pTrc99 $SecA_{linker}$	SecA with $(SAG)_2$(SAAG) after the first N-terminal 20 amino acids	This study

In contrast, the deletion of the N terminus was lethal (Fig. 5*B*). When the SecA (variants) were overexpressed in the same strain, the $SecA_{Linker}$ could largely restore growth, whereas $SecA\Delta N_{20}$ hardly complemented.

To investigate the SecA (variant) activity *in vitro*, an ATPase activity assay in the presence of SecYEG proteoliposomes was performed (Fig. 5*C*). Thereby, the ATPase hydrolysis activity of SecA in the absence (basal ATPase) and the presence of proOmpA (translocation ATPase) was determined by measuring the free phosphate concentration using a malachite green reagent. At low concentrations (50 nM), SecA (variants) barely showed ATPase activity. In the presence of proOmpA the translocation ATPase activity of wild type SecA increased, whereas the mutants were still barely active. Interestingly, at high SecA concentrations (500 nM), $SecA_{Linker}$ performed ATP hydrolysis close to wild type level in the absence and presence of proOmpA.

To further examine the concentration-dependent $SecA_{Linker}$ activity, proOmpA translocation assays were performed with SecYEG proteoliposomes. Translocation of proOmpA into the SecYEG proteoliposomes results in the appearance of proOmpA that is protected against externally added proteinase K. The formation of proteinase K-protected proOmpA is dependent on ATP, whereas the rate of translocation saturates at ~200 nM SecA (Fig. 5*D*). As expected, $SecA\Delta N_{20}$ did not show any translocation activity. However, the SecA with the linker insertion was barely active at nominal SecA concentrations (200 nM), but at very high concentration (~500 nM) was supported proOmpA translocation at rates comparable with those observed with wild type SecA at much lower concentrations.

To investigate the reason for the remarkable concentration-dependent activity of $SecA_{Linker}$, the binding of SecA to SecYEG reconstituted into large nanodiscs was tested (Fig. 5*E*). In comparison with wild type SecA, the binding affinity of $SecA_{Linker}$ is strongly reduced. However, at very high concentration (2 μM), saturation of binding was detected, demonstrating that the linker insertion impacts translocation by reducing the SecA-SecYEG binding affinity. Interestingly, $SecA\Delta N_{20}$ shows a similar reduced binding affinity, but this mutant is also inactive at high concentrations. These data therefore suggest that the lipid interaction of the N terminus of SecA, in addition to tethering the SecA to the membrane, functions by allosterically activating the SecA for high affinity SecYEG binding and ATP hydrolysis.

Discussion

During protein translocation, SecA and SecYEG form a functional interaction unit. A crucial step in this process is the targeting of SecA to the cytoplasmic membrane. Although it has been shown that anionic lipids are crucial for the SecA function (7, 8), the exact role of the lipids has remained elusive. Here, we designed small and large nanodiscs, containing a single copy of SecYEG surrounded by low or high lipid quantities, respectively. The formation of nanodiscs was confirmed by size exclusion chromatography and AFM. It demonstrated that SecYEG and the scaffold protein MSP1E3D1 (for small discs) or ApoE422k (for large discs) eluted in one fraction during the purification. Small discs showed an average diameter of 12.7 nm, which is in good agreement with the 13 nm reported before (13). The large nanodiscs had a size of 31 nm. However, in comparison with the small discs, the size distribution of the large discs was much broader. Considering that MSP1E3D1 always forms a two-copy belt around the lipids, whereas the copy number of ApoE422k can vary, the broader size distribution is not surprising. It has been suggested that the ApoE422k to lipid ratio determines the particle size (15). A previous study by Blanchette *et al.* (25) reported disc sizes ranging from 14 to 33 nm, when a ratio of ApoE422k:lipid of 10:1300 was used. A recent study using the same reconstitution ratio as described in this work (ApoE422k:lipid ratio: 10:1800) reported a monodisperse disc size of 23 nm. However, the disc sizes increased and a broader size distribution was achieved when the lipid composition was changed from POPC to a more complex lipid composition (19). Therefore the disc sizes reported here are in good agreement with early studies.

The SecYEG complex was reconstituted such that according to Poisson distribution a monomeric state was achieved in 16% of the discs, whereas 80% remained empty. It has been reported earlier that the disc size increased when the membrane protein bacteriorhodopsin was reconstituted (25). With bacteriorhodopsin, not only monomeric but also trimeric states were achieved. Here, the presence of reconstituted single SecYEG complexes did not have an effect on the disc size. When measuring the height of the large discs, some discs showed a local increase in height. These height increases have been shown in earlier studies to correspond to the periplasmic and cytoplasmic loop of SecYEG (21). Therefore, the local height increases allowed us to determine the number of discs containing

SecYEG. Approximately 14.5% of the discs showed an increased height representing reconstituted SecYEG complexes, which is in good agreement with the Poisson distribution calculation to determine the reconstitution efficiency. To further assess the oligomeric state of SecYEG in the large discs, a FCCS experiment was performed. Thereby the cross-correlation between differently labeled and reconstituted SecYEG complexes was determined. For large discs the cross-correlation was determined to be less than 10%, which is due to excitation cross-talk and unspecific double-labeling as reported earlier (17). When the SecYEG to ApoE422k ratio was changed from 0.25:10 to 1:10, statistically resulting in 14% of the discs containing multiple copies of SecYEG, a cross-correlation of 50% was detected. Overall, these data are in good agreement with the FCCS experiments performed by Taufik *et al.* (17) demonstrating a monomeric SecYEG state in small discs.

Based on our findings and the resulting average size distribution of the small and large nanodiscs, the single reconstituted SecYEG complexes will be surrounded by ~120 and 1060 phospholipids, respectively. Strikingly, SecYEG complexes present in the small nanodiscs are barely active for protein translocation using a FRET assay reported previously (17). Only at very high SecA concentration, activity is detected. In contrast, the single SecYEG present in the large nanodiscs is active already at the SecA concentrations needed to induce protein translocation in SecYEG proteoliposomes or IMVs. The translocation activity of SecA in the nanodiscs as addressed with a FRET based assay correlates with the ability to bind SecYEG. Although in the large nanodiscs, protein translocation already was detected at 50 nM SecA, very high SecA concentrations were needed to support protein translocation in the small nanodiscs (*i.e.* up to 1 μM). SecYEG present in large nanodiscs showed a K_D for SecA binding of ~300 nM, whereas with the small nanodiscs a K_D of ~3 μM was obtained. The latter is in the same order of magnitude as binding as the K_D of SecA to detergent-solubilized SecYEG (~ 3.9 μM) (10). This poor binding affinity might be explained by several aspects. According to the dimensions of SecYEG, ~20% of the small discs will be occupied by the translocation complex, leaving only a low lipid surface area unoccupied (26). Therefore, the binding of SecA to the disc might be hindered because of spatial interference with SecYEG. This idea is supported by the observation that SecA-empty disc binding curves show a linear increase and, as expected, no saturation. The data imply that SecA binds unspecifically to lipids but specifically to SecYEG. Compared with proteoliposomes, SecYEG large discs still show a lower binding affinity for SecA (1–3 nM *versus* 300 nM, respectively). This difference could suggest that although the disc size was increased, the lipid area is still not large enough to support the most efficient binding. Further, as shown by AFM, only 14.5% of the discs contained a copy of SecYEG. Although not labeled, the remaining 85.5% empty discs can be bound unspecifically by SecA. Even though unspecific binding of SecA to empty discs was only observed at high SecA concentrations, we cannot exclude that lipid binding interfered with the K_D calculations from the MST data. Therefore the calculation yields an apparent K_D. Further, a binding defect could be due to the planar organization of the bilayer in the discs, possibly providing a different lateral lipid pressure as compared with curved liposomes. It is well established that SecA binds acidic phospholipids through its amphipathic N terminus. This region of SecA is known to penetrate the lipid bilayer as shown with Langmuir planar lipid monolayers (6) and membrane vesicles (27). Possibly, a spherical shape of the liposomes favors membrane insertion of the N terminus as compared with the planar nanodiscs bilayers.

To investigate the importance of the lipid composition, SecA binding to SecYEG large discs comprising native *E. coli* lipids was also measured. *E. coli* cytoplasmic membranes contain ~25% PG (28), which is similar to the DOPG concentration of the synthetic lipid mixture used in this study. SecA binding was slightly less efficient when SecYEG was reconstituted into native *E. coli* lipids. No SecA binding was detected when the SecYEG large discs lacked the anionic lipid DOPG, which is consistent with earlier studies showing that this lipid mixture also does not support translocation (7, 8, 23).

Our data support the notion that SecA first needs to bind to acidic phospholipids via ionic interactions with its N terminus before it can bind SecYEG with high affinity. Previously, we have shown that acidic phospholipids form a annulus around the SecYEG channel (29), and we hypothesize that this phenomenon contributes to the SecA binding and activity. The N terminus may have two distinct functions: a membrane tethering and/or an allosteric function, whereby lipid binding induces a conformational change on SecA. In this respect, in the *T. maritima* SecA-SecYEG complex structure, the N terminus of SecA is positioned such that it would not contact the lipid bilayer. It is important to note here that the crystal structure was produced with detergent-solubilized protein in the absence of a membrane. However, as predicted from this structure, at least a 30 Å translational movement of the N terminus of SecA is needed to penetrate the membrane. Given the proximity of the N terminus of SecA to nucleotide binding fold 1, such reallocation is predicted to evoke a conformational change to SecA that may directly affect the ATPase activity and the ability of SecA to binding SecYEG. To discriminate between a sole tethering function and the proposed conformational change or a combination of both, a $SecA_{Linker}$ mutant was constructed that contained a flexible 10 amino acid linker after the first 20 N-terminal residues. This linker should not disrupt the N-terminal tethering function but should no longer or less efficiently be able to inflict the lipid binding-dependent proposed conformational change. Indeed, the activity of $SecA_{Linker}$ was substantially reduced both *in vitro* and *in vivo*, but activity was fully restored when high levels of $SecA_{Linker}$ were used. In contrast, removal of the N-terminal 20 amino acid ($SecA\Delta N_{20}$) rendered SecA essentially inactive even when tested at high concentration, consistent with previous studies (11). Both the $SecA_{Linker}$ and $SecA\Delta N_{20}$ showed a reduced ability to bind SecYEG as compared with the wild type SecA. The residual lipid binding of $SecA\Delta N_{20}$ might relate to the C terminus that has been shown to also bind to lipids (30). Importantly, the observation that high levels of $SecA_{Linker}$ restore the activity is consistent with our proposed allosteric binding mechanism in which SecA is initially recruited to the membrane via a lipid-bound intermediate whereupon it changes its conformation thereby becoming

TABLE 2
Primers used in this study

Primer name	Primer sequence (5′ → 3′)
ABS49	GTAGTAGTAGAGCTCATGCTAATCAAATTGTTAACTAAAG
ABS50	GTAGTAGTATCTAGATTATTGCAGGCGGCCATG
ABS51	GTAGTAGAGCTCATGCATCATCACCACCACCATGGCAGCGGCAGCATGCTAATCAAATTGTTAACTAAAG
ABS52	GTAGTAGTAGAGCTCATGCGCAAAGTGGTCAAC
ABS53	GTAGTAGAGCTCATGCATCATCACCACCACCATGGCAGCGGCAGCATGCGCAAAGTGGTCAAC
ABS54	CACCAATGCTTCTGGCGTCAGG
ABS55	GCCCGCCGCGCTGCCCGCGCTGCCCGCGCTCCGGCGCAGGGTGCGATC
ABS56	AGCGCGGGCAGCGCGGGCAGCGCGGCGGGCATGCGCAAAGTGGTCAAC
ABS57	CAGACCGCTTCTGCGTTCTG

primed for high affinity SecYEG binding. With $SecA_{Linker}$ this priming step is deficient, thus allowing SecYEG binding only with lower affinity, hence the need for high levels of SecA.

To summarize, our study provides evidence for a new mechanism by which SecA binds to the SecYEG complex, wherein SecA binds to negatively charged lipids via its positively charged N terminus leading to a lipid-bound intermediate. This process is associated with a conformational change of SecA that is brought about by penetration of the N terminus of SecA into the lipid membrane. This step is essential for high affinity SecYEG binding and thus the initiation of protein translocation thereby, providing a mechanism that involves the lipid bound SecA as a true intermediate in the translocation cycle. One may speculate that the large lipid surface allows recruitment of SecA at high rates, upon which SecA diffuses over the two-dimensional surfaces and encounters SecYEG. The significantly larger area presented by the lipid surface compared with the SecA-binding area on SecYEG may act as an antenna to kinetically enhance the binding of SecA to SecYEG in a manner reminiscent of the manner with which DNA-binding proteins bind to DNA and diffuse one-dimensionally along the duplex before binding their cognate site (31).

Experimental Procedures

Cloning Procedure—Wild type *secA* and *secA* mutants (Table 1) were generated from pMKL18 (32) and cloned into pTrc99A. Standard cloning techniques were used to generate the N-terminally truncated SecA ($SecA\Delta N_{20}$) that lacks amino acids 1–20. The generation of $secA_{Linker}$, with an $(SAG)_2(SAAG)$ linker inserted after the first 20 N-terminal amino acids, was carried out by overlap PCR using the primers indicated in Table 2.

In Vivo Complementation Assay—Plasmids encoding for wild type SecA, $SecA\Delta N_{20}$, and $SecA_{Linker}$ were transformed into the *secATs* mutant strain *E. coli* BL21.19 and tested for the ability to complement the SecA deficiency by growing on LB plates at nonpermissive temperatures as described previously (33). For overexpression, plates were supplemented with 10 μM isopropyl 1-thio-β-D-galactopyranoside.

Protein Production and Purification—E. coli BL21 (DE3) harboring wild type SecA or SecA mutants, designed in this study, was grown at 37 °C to an A_{600} of 0.6, whereupon protein expression was induced by addition of 0.5 mM isopropyl 1-thio-β-D-galactopyranoside. After 2 h of growth, the cells were harvested at 6000 x *g* for 15 min at 4 °C, resuspended in 25 mM HEPES/KOH, pH 6.5, and stored at −80 °C. SecA was purified as described before (34).

The proOmpA derivative fused to dihydrofolate reductase (proOmpA-DHFR) was overexpressed from pET504 in *E. coli* DH5α, purified from inclusion bodies, and stored in 8 M urea as described previously (35). ProOmpA-DHFR harboring a cysteine mutation at position 282 in the OmpA domain was labeled with Cy3. Free dye was removed by TCA precipitation.

SecYEG was overexpressed in *E. coli* SF100 and purified from IMVs as described before (35). Briefly, IMVs were solubilized with 2% *n*-dodecyl β-D-maltoside for 30 min in the presence of 1 Complete Protease inhibitor tablet (Roche). The solubilized membranes were incubated with Ni^+-NTA beads (Qiagen) for 2 h and transferred to a Bio-spin micro column (Bio-Rad). The column was washed with 6 column volumes of a washing buffer containing 50 mM phosphate buffer, pH 7, 100 mM KCl, 0.1% *n*-dodecyl β-D-maltoside, 10 mM imidazole, and 20% glycerol. The Ni^+-NTA-bound SecYEG was labeled with 600 μM of either Atto647N, Alexa 488 or Cy5 for 2 h at 4 °C. The labeling procedure was performed at pH 7 to ensure a higher labeling specificity and efficiency. Free dye was removed by extensive washing with washing buffer. SecYEG was eluted with 300 mM imidazole. The purity and concentration of SecYEG and the fluorophores were estimated by SDS-PAGE and spectrophotometrically. The extinction coefficient used for SecYEG at 280 nm was 71,000 M^{-1} cm^{-1}. The extinction coefficients for the fluorophores were used as provided by the manufacturers.

The expression clone to produce the scaffold protein ApoE422k representing an N-terminal 22-kDa fragment of the human apolipoprotein E4, harboring a His_6 and thioredoxin tag was kindly provided by Prof. James Rothman (Yale University, New Haven, CT). ApoE422k was produced and purified as described (19). MSP1E3D1 was kindly provided by Prof. Stephan Sligar (University of Illinois, Urbana, IL) and produced and purified as previously reported (36).

Reconstitution of SecYEG into Proteoliposomes—A lipid mixture containing DOPC:DOPG:DOPE (molar ratio 40:30:30) or DOPC:DOPE (molar ratio 40:60) (Avanti Biochemicals, Birmingham, AL) (100 μl; 4 mg/ml) was solubilized with 0.5% Triton X-100 and mixed with 2.5 nmol of purified SecYEG. Reconstitution was performed as described before (37).

Nanodisc Reconstitution of SecYEG—For nanodisc formation, a lipid mixture containing DOPC:DOPG:DOPE (molar ratio 40:30:30), DOPC:DOPE (molar ratio 40:60), or *E. coli* phospholipids (Avanti Biochemicals) was dried in a vacuum evaporator. Remaining traces of chloroform were removed by further drying of the lipid film in a desiccator overnight. Lipids were resuspended in a buffer containing 23 mM sodium cholate,

25 mM HEPES/KOH, pH 7.4, 140 mM KCl, 0.17 mM DTT. For small nanodisc formation, SecYEG, MSP1E3D1, and lipids were mixed in a molar ratio of 1:10:250. Large nanodiscs were produced by mixing SecYEG, ApoE422k, and lipids at a molar ratio of 0.25:10:1800. The reconstitution mixtures were incubated at 4 °C for 1 h. Detergent was removed using Bio-Beads SM2 sorbent (Bio-Rad) in an overnight step. Minor amounts of formed proteoliposomes were removed by a centrifugation at 250,000 × *g* for 30 min. Nanodiscs were subjected to size exclusion chromatography by fast protein liquid chromatography using a Superose 6 column (GE Healthcare), and 0.5-ml elution fractions were collected in 50 mM HEPES/KOH (pH 7.4), 100 mM KCl, and 5% glycerol. Nanodisc containing fractions were analyzed by SDS-PAGE.

In Vitro proOmpA Translocation Assay—The activities of wild type and mutated SecA were analyzed by a standard proOmpA translocation and protease protection assay (38).

ATPase Activity Assay—ATPase activity assay of SecA was performed with minor modifications as described before (7, 39). A reaction mixture containing 25 mM HEPES/KOH, pH 7.4, 25 mM KCl, 5 mM $MgCl_2$, 0.1 mg/ml BSA, 2 mM DTT, 0.04 mg/ml SecB, 5 μM SecYEG proteoliposomes, and 50 or 500 nM wild type or mutated SecA was prepared. To measure the proOmpA-dependent SecA activity, proOmpA was added to a final concentration of 0.04 mg/ml. The basal SecA activity was measured by adding an 8 M urea buffer instead of proOmpA. Reactions were initiated by addition of 5 mM ATP and performed at 37 °C for 30 min. Following, samples were diluted to reach an ATP concentrations below 0.25 mM. Free phosphate was quantified using a Malachite Green Phosphate assay kit (Gentaur).

Atomic Force Microscopy—Nanodiscs were diluted in a buffer containing 50 mM HEPES/KOH, pH 7.4, 50 mM KCl, 5% glycerol, and 100 mM $MgCl_2$ to a final concentration of ~1 nM. By incubation of this solution for 10 min with freshly cleaved mica, the nanodiscs were immobilized on the surface. Nonimmobilized material was rinsed off. AFM images were recorded in tapping mode in ScanAsyst-fluid regime by a Multimode 8 instrument, Controller V (Bruker). Images were taken using SNL-A silicon probes with a reflective Au coating on the back side and a tip radius of 2 nm. All images were obtained in buffer at room temperature using a spring constant of 0.35 N/m. A 2 kHz tapping frequency was used with a scan size of 3 μm, a scan speed of 0.2 Hz, and a 1024 lines/sample resolution capability. Analysis of height and diameter of the recorded images was performed manually using NanoScopeAnalysis 1.2 software.

Microscale Thermophoresis—Microscale thermophoresis experiments were performed using a Monolith NT.115 from Nanotemper Technologies (Munich, Germany) to assess the binding of SecA to the SecYEG containing nanodiscs. A serial dilution of unlabeled SecA or a SecA mutant was prepared using a buffer containing 50 mM HEPES/KOH, pH 7.4, 50 mM KCL, 5% glycerol, and 0.5 mg/ml BSA. Cy 5-labeled SecYEG reconstituted in either small or large nanodiscs, and ATP was added to a final concentration of 50 nM and 5 mM, respectively. The samples were loaded into Monolith NT.115 series MST premium coated capillaries, and MST measurements were performed using 80% LED power and 80% IR-laser power. The data were fitted using the Hill equation.

FRET Measurements—FRET assays to examine protein translocation into SecYEG reconstituted nanodiscs were performed using SLM2 spectrofluorometer (Aminco Bowmann), as described previously (16). Briefly, proOmpA-DHFR was labeled with Cy3-maleimide (donor) (λ_{EX} = 550, λ_{EM} = 570), and the DHFR domain was folded in the presence of methotrexate and NADPH. $SecY_{C148}EG$ was labeled with Atto647N (acceptor) (λ_{EX} = 650, λ_{EM} = 670). FRET-based real time translocation of 200 nM prefolded proOmpA-DHFR-Cy3 was performed in the presence of 200 nM $SecY_{C148}EG$-Atto647N reconstituted small or large nanodiscs, 50 mM HEPES/KOH, pH 7.4, 30 mM KCL, 5 mM $MgCl_2$, and 10 mM DTT. Translocation was initiated with 5 mM ATP, whereby the donor fluorophore was excited at 525 nm, and FRET efficiency was measured as an increase in acceptor fluorescence at 670 nm.

Fluorescence Cross-correlation Spectroscopy—FCCS experiments were performed on a dual color laser scanning LSM710 inverted confocal microscope (Zeiss). A helium-neon laser at 488 nm and an argon laser at 633 nm were used to excite the fluorophore-conjugated $SecY_{C148}EG$. The fluorescence was recorded in blue (505–570 nm) and red (640–700 nm) channels. $SecY_{C148}EG$ was labeled with Atto647N and AF488 simultaneously (17, 18). The labeling efficiency for each fluorophore reached ~55%, resulting in a 110% overall labeling efficiency. This slight overlabeling suggests a small amount of unspecific labeling. Fluorescently labeled $SecY_{C148}EG$ was reconstituted into large nanodiscs. Autocorrelation in fluorescence for both fluorophores was recorded and analyzed as described before (40).

Author Contributions—S. K. designed and performed most of the experiments, analyzed the results, and wrote the paper. J. D. W. conducted the cloning and *in vivo* activity assays. I. V. and J. P. B. designed and conducted experiments that provided the basis of the work. P. G. preformed atomic force microscopy experiments and was supervised by A. H. A. J. M. D. and A. M. V. O. conceived the idea for the project, designed the experiments, supervised the work, and wrote the paper. All authors contributed to the editing of the manuscript and approved the final version.

Acknowledgments—We thank M. Exterkate, I. Kusters, and A. B. Seinen for technical support and many valuable comments and discussions on the project.

References

1. Driessen, A. J., and Nouwen, N. (2008) Protein translocation across the bacterial cytoplasmic membrane. *Annu. Rev. Biochem.* **77,** 643–667
2. Driessen, A. J. (2001) SecB, a molecular chaperone with two faces. *Trends Microbiol.* **9,** 193–196
3. Vrontou, E., and Economou, A. (2004) Structure and function of SecA, the preprotein translocase nanomotor. *Biochim. Biophys. Acta* **1694,** 67–80
4. Zimmer, J., Nam, Y., and Rapoport, T. A. (2008) Structure of a complex of the ATPase SecA and the protein-translocation channel. *Nature* **455,** 936–943
5. Cunningham, K., Lill, R., Crooke, E., Rice, M., Moore, K., Wickner, W., and Oliver, D. (1989) SecA protein, a peripheral protein of the *Escherichia coli* plasma membrane, is essential for the functional binding and translocation of proOmpA. *EMBO J.* **8,** 955–959

6. Breukink, E., Demel, R. A., de Korte-Kool, G., and de Kruijff, B. (1992) SecA insertion into phospholipids is stimulated by negatively charged lipids and inhibited by ATP: A monolayer study. *Biochemistry* **31,** 1119–1124
7. Lill, R., Dowhan, W., and Wickner, W. (1990) The ATPase activity of SecA is regulated by acidic phospholipids, SecY, and the leader and mature domains of precursor proteins. *Cell* **60,** 271–280
8. Hendrick, J. P., and Wickner, W. (1991) SecA protein needs both acidic phospholipids and SecY/E protein for functional high-affinity binding to the *Escherichia coli* plasma membrane. *J. Biol. Chem.* **266,** 24596–24600
9. Wu, Z. C., de Keyzer, J., Kedrov, A., and Driessen, A. J. (2012) Competitive binding of the SecA ATPase and ribosomes to the SecYEG translocon. *J. Biol. Chem.* **287,** 7885–7895
10. Robson, A., Gold, V. A., Hodson, S., Clarke, A. R., and Collinson, I. (2009) Energy transduction in protein transport and the ATP hydrolytic cycle of SecA. *Proc. Natl. Acad. Sci. U.S.A.* **106,** 5111–5116
11. Bauer, B. W., Shemesh, T., Chen, Y., and Rapoport, T. A. (2014) A "push and slide" mechanism allows sequence-insensitive translocation of secretory proteins by the SecA ATPase. *Cell.* **157,** 1416–1429
12. Floyd, J. H., You, Z., Hsieh, Y.-H., Ma, Y., Yang, H., and Tai, P. C. (2014) The dispensability and requirement of SecA N-terminal aminoacyl residues for complementation, membrane binding, lipid-specific domains and channel activities. *Biochem. Biophys. Res. Commun.* **453,** 138–142
13. Denisov, I. G., Baas, B. J., Grinkova, Y. V., and Sligar, S. G. (2007) Cooperativity in cytochrome P450 3A4: linkages in substrate binding, spin state, uncoupling, and product formation. *J. Biol. Chem.* **282,** 7066–7076
14. Dong, J., Peters-Libeu, C. A., Weisgraber, K. H., Segelke, B. W., Rupp, B., Capila, I., Hernáiz, M. J., LeBrun, L. A., and Linhardt, R. J. (2001) Interaction of the N-terminal domain of apolipoprotein E4 with heparin. *Biochemistry* **40,** 2826–2834
15. Blanchette, C. D., Law, R., Benner, W. H., Pesavento, J. B., Cappuccio, J. A., Walsworth, V., Kuhn, E. A., Corzett, M., Chromy, B. A., Segelke, B. W., Coleman, M. A., Bench, G., Hoeprich, P. D., and Sulchek, T. A. (2008) Quantifying size distributions of nanolipoprotein particles with single-particle analysis and molecular dynamic simulations. *J. Lipid Res.* **49,** 1420–1430
16. Kedrov, A., Kusters, I., Krasnikov, V. V., and Driessen, A. J. (2011) A single copy of SecYEG is sufficient for preprotein translocation. *EMBO J.* **30,** 4387–4397
17. Taufik, I., Kedrov, A., Exterkate, M., and Driessen, A. J. (2013) Monitoring the activity of single translocons. *J. Mol. Biol.* **425,** 4145–4153
18. Kedrov, A., Sustarsic, M., de Keyzer, J., Caumanns, J. J., Wu, Z. C., and Driessen, A. J. (2013) Elucidating the native architecture of the YidC: ribosome complex. *J. Mol. Biol.* **425,** 4112–4124
19. Bello, O. D., Auclair, S. M., Rothman, J. E., and Krishnakumar, S. S. (2016) Using ApoE-nanolipoprotein particles to analyze SNARE-induced fusion pores. *Langmuir* **32,** 3015–3023
20. Ramadurai, S., Duurkens, R., Krasnikov, V. V., and Poolman, B. (2010) Lateral diffusion of membrane proteins: consequences of hydrophobic mismatch and lipid composition. *Biophys. J.* **99,** 1482–1489
21. Sanganna Gari, R. R., Frey, N. C., Mao, C., Randall, L. L., and King, G. M. (2013) Dynamic structure of the translocon SecYEG in membrane: direct single molecule observations. *J. Biol. Chem.* **288,** 16848–16854
22. Dickey, A., and Faller, R. (2008) Examining the contributions of lipid shape and headgroup charge on bilayer behavior. *Biophys. J.* **95,** 2636–2646
23. van der Does, C., Swaving, J., van Klompenburg, W., and Driessen, A. J. (2000) Non-bilayer lipids stimulate the activity of the reconstituted bacterial protein translocase. *J. Biol. Chem.* **275,** 2472–2478
24. Keller, R. C., Snel, M. M., de Kruijff, B., and Marsh, D. (1995) SecA restricts, in a nucleotide-dependent manner, acyl chain mobility up to the center of a phospholipid bilayer. *FEBS Lett.* **358,** 251–254
25. Blanchette, C. D., Cappuccio, J. A., Kuhn, E. A., Segelke, B. W., Benner, W. H., Chromy, B. A., Coleman, M. A., Bench, G., Hoeprich, P. D., and Sulchek, T. A. (2009) Atomic force microscopy differentiates discrete size distributions between membrane protein containing and empty nanolipoprotein particles. *Biochim. Biophys. Acta* **1788,** 724–731
26. Frauenfeld, J., Gumbart, J., Sluis, E. O., Funes, S., Gartmann, M., Beatrix, B., Mielke, T., Berninghausen, O., Becker, T., Schulten, K., and Beckmann, R. (2011) Cryo-EM structure of the ribosome-SecYE complex in the membrane environment. *Nat. Struct. Mol. Biol.* **18,** 614–621
27. Ulbrandt, N. D., London, E., and Oliver, D. B. (1992) Deep penetration of a portion of *Escherichia coli* SecA protein into model membranes is promoted by anionic phospholipids and by partial unfolding. *J. Biol. Chem.* **267,** 15184–15192
28. Morein, S., Andersson, A., Rilfors, L., and Lindblom, G. (1996) Wild-type *Escherichia coli* cells regulate the membrane lipid composition in a "window" between gel and non-lamellar structures. *J. Biol. Chem.* **271,** 6801–6809
29. Prabudiansyah, I., Kusters, I., Caforio, A., and Driessen, A. J. (2015) Characterization of the annular lipid shell of the Sec translocon. *Biochim. Biophys. Acta* **1848,** 2050–2056
30. Breukink, E., Nouwen, N., van Raalte, A., Mizushima, S., Tommassen, J., and de Kruijff, B. (1995) The C terminus of SecA is involved in both lipid binding and SecB binding. *J. Biol. Chem.* **270,** 7902–7907
31. Tafvizi, A., Mirny, L. A., and van Oijen, A. M. (2011) Dancing on DNA: kinetic aspects of search processes on DNA. *ChemPhysChem* **12,** 1481–1489
32. Klose, M., Schimz, K. L., van der Wolk, J., Driessen, A. J., and Freudl, R. (1993) Lysine 106 of the putative catalytic ATP-binding site of the *Bacillus subtilis* SecA protein is required for functional complementation of *Escherichia coli* secA mutants *in vivo*. *J. Biol. Chem.* **268,** 4504–5410
33. Wang, H., Na, B., Yang, H., and Tai, P. C. (2008) Additional *in vitro* and *in vivo* evidence for SecA functioning as dimers in the membrane: dissociation into monomers is not essential for protein translocation in *Escherichia coli*. *J. Bacteriol.* **190,** 1413–1418
34. Prabudiansyah, I., Kusters, I., and Driessen, A. J. (2015) *In vitro* interaction of the housekeeping SecA1 with the accessory SecA2 protein of *Mycobacterium tuberculosis*. *PLoS One* **10,** e0128788
35. van der Does, C., de Keyzer, J., van der Laan, M., and Driessen, A. J. (2003) Reconstitution of purified bacterial preprotein translocase in liposomes. *Methods Enzymol.* **372,** 86–98
36. Ritchie, T. K., Grinkova, Y. V., Bayburt, T. H., Denisov, I. G., Zolnerciks, J. K., Atkins, W. M., and Sligar, S. G. (2009) Reconstitution of membrane proteins in phospholipid bilayer nanodiscs. *Methods Enzymol.* **464,** 211–231
37. van der Laan, M., Houben, E. N., Nouwen, N., Luirink, J., and Driessen, A. J. (2001) Reconstitution of Sec-dependent membrane protein insertion: nascent FtsQ interacts with YidC in a SecYEG-dependent manner. *EMBO Rep.* **2,** 519–523
38. Bol, R., de Wit, J. G., and Driessen, A. J. (2007) The active protein-conducting channel of *Escherichia coli* contains an apolar patch. *J. Biol. Chem.* **282,** 29785–29793
39. Lanzetta, P. A., Alvarez, L. J., Reinach, P. S., and Candia, O. A. (1979) An improved assay for nanomole amounts of inorganic phosphate. *Anal. Biochem.* **100,** 95–97
40. Bacia, K., and Schwille, P. (2007) Practical guidelines for dual-color fluorescence cross-correlation spectroscopy. *Nat. Protoc.* **2,** 2842–2856
41. Hanahan, D. (1983) Studies on transformation of *Escherichia coli* with plasmids. *J. Mol. Biol.* **166,** 557–580
42. Baneyx, F., and Georgiou, G. (1990) *In vivo* degradation of secreted fusion proteins by the *Escherichia coli* outer membrane protease OmpT. *J. Bacteriol.* **172,** 491–494
43. Studier, F. W., and Moffatt, B. A. (1986) Use of bacteriophage T7 RNA polymerase to direct selective high-level expression of cloned genes. *J. Mol. Biol.* **189,** 113–130
44. Mitchell, C., and Oliver, D. (1993) Two distinct ATP-binding domains are needed to promote protein export by *Escherichia coli* SecA ATPase. *Mol. Microbiol.* **10,** 483–497